A Metamaterial-Inspired Temperature Stable Inkjet-Printed Microfluidic-Tunable Bandstop Filter

W. Su*, C. Mariotti†, B. S. Cook*, S. Lim‡, L. Roselli† and M. M. Tentzeris*
*School of Electrical and Computer Engineering, Georgia Institute of Technology, Atlanta, Georgia, USA
†Department of Engineering, University of Perugia, Perugia, Italy
‡School of Electrical and Electronics Engineering, Chung-Ang University, Seoul, South Korea

***Abstract*—A low-cost and disposable microfluidic-tunable bandstop filter is presented which is fabricated utilizing a novel inkjet-printing based microfluidics platform. The proposed bandstop filter is based on a split-ring-resonator (SRR) unit cell embedded within the ground of a co-planar waveguide (CPW) transmission line. By loading the capacitive gap of the SRR with an array of fluids with different permittivities, the resonant frequency of the resonator can be tuned over a wide bandwidth. Utilizing only $6\,\mu$L of fluid, which is approximately one twentieth of a drop of water, a $30\,\%$, or $0.4\,\%/\varepsilon_r$ change in resonant frequency can be achieved which is higher than current cleanroom-fabricated microfluidic RF devices in the literature. The high temperature stability of the low-cost microfluidic filter is presented, which demonstrates below $1\,\%$ variance in resonant frequency for operating temperatures ranging from $273\,$K to $332\,$K.**

I. Introduction

Microfluidics have become an invaluable tool over the past decade to manipulate, analyze, and interact with extremely small quantities of liquid in applications such as blood analysis, bio-assays, in-vitro wireless monitoring, manufacturing control, and recently introduced fluid-tunable electronic components [1]. Before the use of microfluidic systems, processes such as bio-assays and water quality analysis required large amounts of liquid ranging from milliliters to several liters, the majority of which is wasted in dead volume required to fill tubing and valves, and never utilized for analysis or measurement purposes. Microfluidics, however, allows fluid analysis to be performed on samples which are micro or nanoliters in volume due to the monolithic integration of sensing and interface electronics, fluidic manipulation structures, and micron sized fluid channels on a single packaged system.

Until recently, microfluidic systems with embedded electronics were fabricated utilizing cleanroom processes as low cost microfluidic fabrication methods did not have viable methods of depositing the embedded electronics in a low-cost manner [2]–[4]. As cleanroom fabrication methods were required, the price point of microfluidic systems was rather high. However, Cook et al. recently demonstrated a microfluidics fabrication platform which can fabricate low-cost, disposable microfluidic systems with embedded electronics using an inkjet-printing based fabrication process [1]. Inkjet printing is a rapid and additive fabrication process that can deposit a wide variety of materials, including metals, dielectrics, and nanomaterial-based sensors, at a low cost and with negligible material waste on virtually any substrate [5]–[9].

Cook et al. have demonstrated simple microfluidic tunable and sensing RF systems utilizing this fabrication platform including varactors, microstrip resonators, and antennas [1]. This work aims to extend on previous works and demonstrate a fluid-tunable metamaterial-inspired SRR CPW bandstop filter which will form the basis for future fluid tunable metasurfaces fabricated with this process. Previous demonstrations of fluid-tunable metasurfaces in the literature utilize macro fluidics and have given little attention to characterizing their thermal stability and repeatability. Gordon et al. have demonstrated a fluid tunable metasurface utilizing macro fluidics which achieves a $5.2\,\%$ tuning range over a change in fluid permittivity ranging from 1 to 73 [10]. This work aims to demonstrate unit cell performance of a metasurface utilizing a band-stop filter design with tuning ranges of up to $30\,\%$, as well as characterize the repeatability and temperature stability of the fabricated microfluidic RF device.

II. Fabrication Process

The unit-cell bandstop filter is fabricated utilizing the process shown in Fig. 1. The materials printer utilized for the fabrication process is the Dimatix DMP-2831 (Fujifilm Dimatix, Santa Clara, CA, USA). The first step in the process involves patterning a $2\,\mu$m thick metallization layer on the host substrate, a $230\,\mu$m thick Kodak photo paper (Office Depot, Atlanta, GA, USA), utilizing ANP Silver-Jet 55LT-25C silver nanoparticle ink (Advanced Nano Products, Sejong, Korea). After printing the metallization layer, it is cured for 30 min at $120\,^\circ$C to produce a bulk metallization with a conductivity of $1.3e7\,$S/m [5]. Subsequently, a $15\,\mu$m thick polymer adhesion layer is printed on top of the metallization utilizing an SU-8 polymer ink (Microchem, Newton, MA, USA) which will enable the bonding and sealing of the microfluidic channels onto the host substrate. To create the microfluidic channels, a second $1.5\,$mm thick poly(methyl-methacrylate) (PMMA) substrate (McMaster-Carr, Atlanta, GA, USA) is laser etched to produce the micron-sized channels and fluid inlets/outlets using an Epilog Legend EXT 120W laser (Epilog Laser, Golden, CO, USA). Bonding is carried out by flipping the substrate housing the channels onto the host substrate and applying $10\,\mathrm{N/cm^2}$ of force while bringing the entire structure up to $80\,^\circ$C. The finished system is then allowed to cool while still under pressure to mitigate warping due to the unequal thermal expansion coefficients between the two substrates.

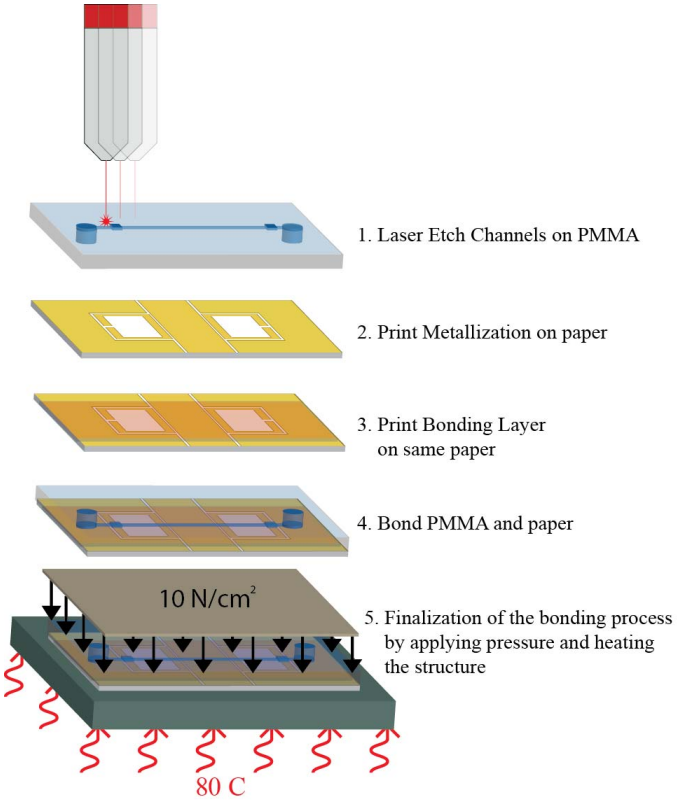

Fig. 1. Fabrication process.

III. Theory of Operation

The tunable band-stop filter is based on the SRR, which is a commonly used metasurface unit cell as it is simple to fabricate and model. The SRR unit cell can be modeled as a series R-L-C as shown in Fig. 2, where R represents a parasitic loss, L is the loop inductance, and C the gap capacitance.

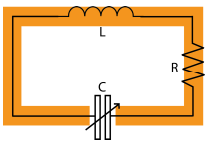

Fig. 2. Equivalent circuit of the SRR unit cell.

The resonate frequency of SRR can be calculated by Eq. 1. The gap capacitance in the SRR is the critical component in the fluid tunable bandstop filter as a fluid channel can be easily run over the gap. When liquids of different permittivity are present over the gap, the capacitance of the gap changes due to changes in the displacement field strength. This leads to a change in the resonant frequency of the SRR.

$$f = \frac{1}{(2\pi\sqrt{LC})} \tag{1}$$

By closely coupling the SRR to the CPW line, energy transfer occurs from the line to the resonator near the resonant

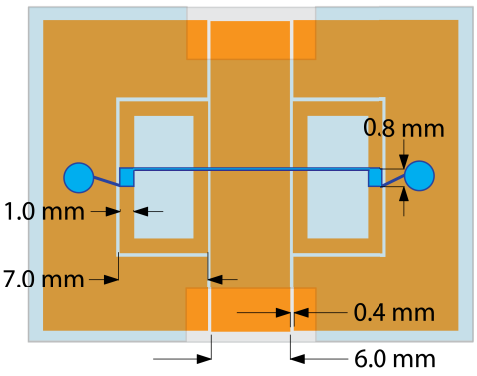

(a) Geometry

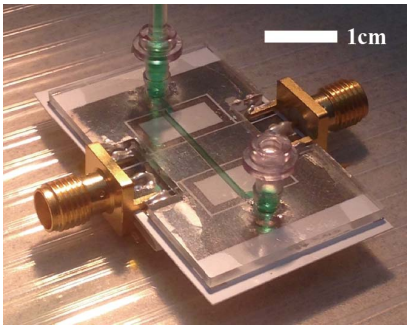

(b) Photograph

Fig. 3. Geometry (a) and photograph (b) of the proposed SRR bandstop filter.

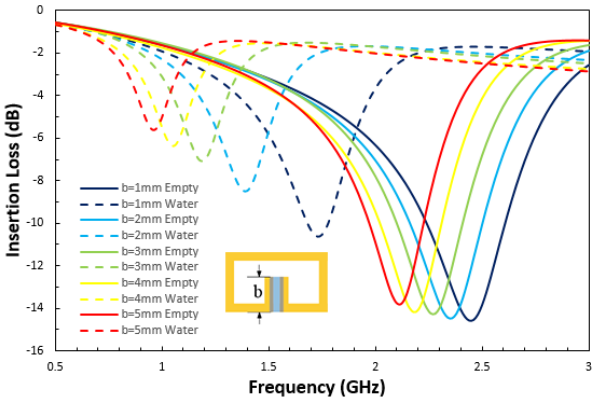

Fig. 4. Sensitivity change with different slot in simulation.

frequency. The coupled energy experiences a phase shift from the resonator which, when coupled back to the line destructively interferes with the forward going wave. This causes a band-stop effect. The coupling factor, and SRR unit cell size are optimized in the HFSS frequency domain solver for a center frequency of 2.4 GHz and input impedance of 50 Ω when the capacitive gap is loaded with air. The optimized design can be seen in Fig. 3.

For the sake of investigating suitable sensitivity, different slot size is simulated. As shown in Fig. 4, Sensitivity grow with b, while the strength of resonate decreasing. The best sensitivity in Fig. 4. is $0.8\,\%/\varepsilon_r$ when b is 5 mm. But the insertion loss for b=5 with water filled is only -6 dB, which shows a limited tunable range. This set of simulation demonstrates the possibility of developing a super sensitive sensor for low permittivity fluid. However, since water is the most common fluid and has a relatively high permittivity, a large sensitive range is need. Finally, 1 mm slot length is chosen for fabricated and measured for nice bandstop ability.

IV. Measurement Results

Following the fabrication of the proposed band-stop filter, the measured and simulated results of the band-stop filter are reported with a focus on two critical components: the sensitivity, or change in resonant frequency of the filter versus the permittivity of the fluid present in the channel, and the repeatability and temperature stability of the device.

To measure the proposed filter, SMA connectors are mounted utilizing Chemtronics CW2460 two part conductive silver epoxy (Circuit Works, Wilmington, NC, USA). The device is then mounted in a temperature controlled chamber, and connected to fluid feed lines which feed the various fluids through the microfluidic filter. A Rhode and Schwartz ZVA-8 VNA is used to measure the S-parameters of the device under varying fluid and temperature conditions.

A. Sensitivity Measurement

The first test introduces fluids with permittivities ranging from 1 to 73 including air, hexanol, glycerol, and deionized (DI) water at room temperature to determine the sensitivity of the device. The permittivities of these fluids at 2.4 GHz can be found in Table I.

TABLE I. Permittivity of Tested Fluids at 2.4 GHz [11]–[13].

Name	Permittivity	
	Real part	Imaginary Part
Hexanol	3	2.5
Glycerol	4	0.4
Water	73	8

In Fig. 5, the comparison between simulated and measured Insertion Loss (IL) of the band-stop filter is shown for the various fluids. It can be seen that when the channel is filled with air, the resonant frequency of the filter is 2.4 GHz which is in good agreement with the simulation results. The pass-band is above -2 dB both below and above the resonant frequency. As higher permittivity fluids are introduced, the resonant frequency of the filter decreases all the way to 1.74 GHz with the introduction of water. This is a 28 % change in resonant frequency, or approximately $0.4\,\%/\varepsilon_r$. The highest current sensitivity of cleanroom-fabricated microfluidic RF devices in the literature is approximately $0.25\,\%/\varepsilon_r$, which was demonstrated by Chretiennot et al. [14]. The 3 dB bandwidth of the filter ranging from empty, to filled with hexanol, glycerol and water are 8.3 %, 8.5 %, 13 %, and 12.6 %, respectively.

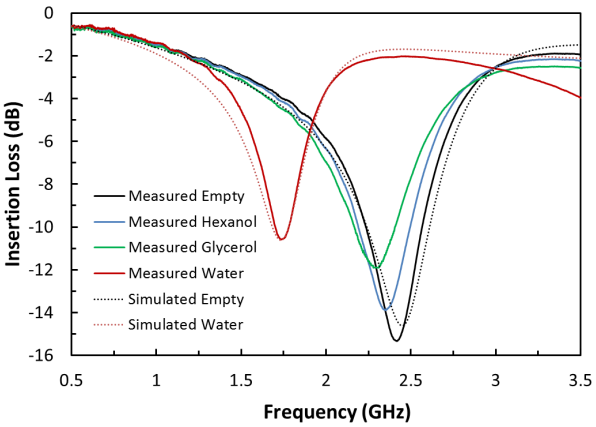

Fig. 5. Measured and simulated Insertion Loss (IL) for different fluids pumped into the channel.

The simulated and measured sensitivities of the device are reported in Fig. 6, showing very good agreement between the simulated and measured results. The sensitivity curve shows a highly linear trend which is optimal for sensing. Typically, microfluidic-tunable RF devices demonstrate a logarithmic sensitivity curve [1].

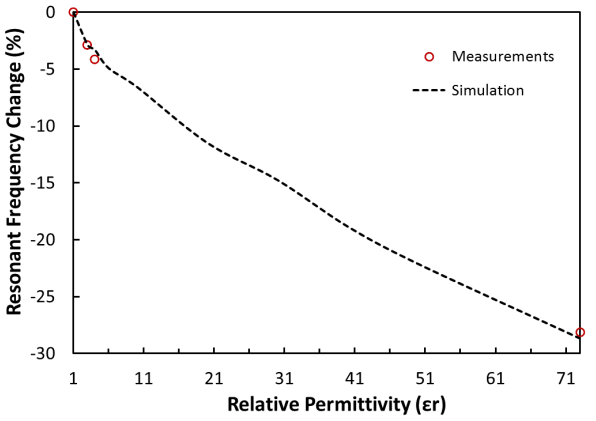

Fig. 6. Resonance frequency shift (in percentage) due to different fluids in the channel.

B. Temperature Stability Measurement

Typical devices have a temperature range in which they optimally perform. In the case of these disposable microfluidic RF devices, it is important to quantify stability versus variation in temperature. This is even more important in fluid-tunable or sensing systems as there will not only be temperature variation of the system itself, but typical fluids experience a drastic change in permittivity over temperature [15].

As a calibration, the system is initially filled with air, and the temperature of the test chamber is raised from room temperature, or 297 K, to 332 K (23 to 60 °C). The S-parameters of the filter are recorded along with the steady state

temperature within the chamber. The results of the calibration test, displayed in Fig. 7 show that the resonant frequency of the system experiences less than $1\,\%$ variance over a the temperature range of $297\,\mathrm{K}$ to $332\,\mathrm{K}$. Upon returning to room temperature, the resonant frequency returns to its initial value as well. This variance can therefore be calibrated out of the final measurement result in practical systems.

The microfluidic filter performs well over temperature when empty, however, many fluids have a temperature-dependent permittivity. Water is known to have a relatively large change in permittivity over temperature. Catenaccio report a decrease of 21% in permittivity from $297\,\mathrm{K}$, to $332\,\mathrm{K}$ [15]. To measure this effect on the bandstop filter, the microfluidic channel is filled with water, and the temperature is then raised from $297\,\mathrm{K}$, to $332\,\mathrm{K}$, allowing the device to reach steady state before moving to the next temperature. It can be seen in Fig. 7 that the resonant frequency shift when the resonator is loaded with water increases approximately $9\,\%$ over the temperature range due to the decrease in permittivity of the water. Using the results from the sensitivity measurement in Fig. 6, which yields a change of $0.4\,\%/\varepsilon_r$, along with the reported $21\,\%$ change in permittivity of water over the measured temperature range, an $8.4\,\%$ change is expected which matches very closely with the measured $9\,\%$ change. These extremely promising results show that the device can not only be used as a tunable filter, but also a temperature sensor. Again, the resonant frequency returns to its original value when the device returns to room temperature.

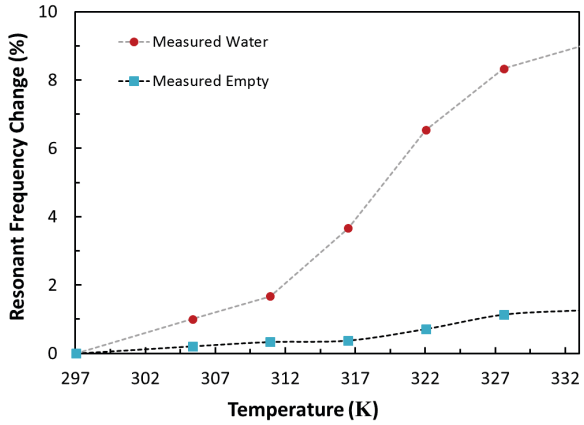

Fig. 7. Resonance frequency shift (in percentage) due to temperature change.

V. Conclusion

A bandstop microfluidic tunable metamaterial-inspired filter utilizing a low-cost inkjet-printed microfluidics platform is demonstrated that has a high sensitivity of $0.4\,\%/\varepsilon_r$ - nearly double that of cleanroom-fabricated microfluidic RF devices in the literature. The fabricated filter demonstrates a high level of temperature stability with a variance in resonant frequency below $1\,\%$ over the temperature range of $297\,\mathrm{K}$, to $332\,\mathrm{K}$. The use of the filter as a temperature sensor is also demonstrated in which a $9\,\%$ increase in resonant frequency is shown as the device temperature is increased from $297\,\mathrm{K}$, to $332\,\mathrm{K}$. These results are directly confirmed by the measured sensitivity of the device, and the expected change in permittivity of water due to temperature. The initial results will be extended to creating fluid-tunable SRR metasurfaces which can be used in a vast array of applications ranging from in-vivo sensing, to wide-range tunable RF filters.

References

[1] B. Cook, J. Cooper, and M. Tentzeris, "An inkjet-printed microfluidic rfid-enabled platform for wireless lab-on-chip applications," *Microwave Theory and Techniques, IEEE Transactions on*, vol. 61, no. 12, pp. 4714–4723, Dec 2013.

[2] A. W. Martinez, S. T. Phillips, B. J. Wiley, M. Gupta, and G. M. Whitesides, "Flash: A rapid method for prototyping paper-based microfluidic devices," *Lab on a Chip*, vol. 8, pp. 2146–2150, 2008.

[3] H. Klank, J. P. Kutter, and O. Geschke, "Co2-laser micromachining and back-end processing for rapid production of pmma-based microfluidic systems," *Lab on a Chip*, vol. 2, pp. 242 – 246, 2002.

[4] P. K. Yuen and V. N. Goral, "Low-cost rapid prototyping of flexible microfluidic devices using a desktop digital craft cutter," *Lab on a Chip*, vol. 10, pp. 384–387, 2010.

[5] B. S. Cook and A. Shamim, "Inkjet printing of novel wideband and high gain antennas on low-cost paper substrate," *IEEE Transactions on Antennas and Propagation*, vol. 60, pp. 4148 – 4156, 2012.

[6] B. S. Cook, J. R. Cooper, and M. M. Tentzeris, "Multi-layer rf capacitors on flexible substrates utilizing inkjet printed dielectric polymers," *IEEE Microwave Component Letters*, vol. 23, pp. 353 – 355, 2013.

[7] T. Le, V. Lakafosis, Z. Lin, C. P. Wong, and M. M. Tentzeris, "Inkjet-printed graphene-based wireless gas sensor modules," in *Procs. IEEE 62nd ECTC Conference*, 2012, pp. 1003 – 1008.

[8] L. Yang, A. Rida, and M. M. Tentzeris, "Design and development of radio frequency identification (rfid) and rfid-enabled sensors on flexible low cost substrates," *Synthesis Lectures on RF/Microwaves*, vol. 1, pp. 1–89, 2009.

[9] L. Yang, A. Rida, R. Vyas, , and M. M. Tentzeris, "Rfid tag and rf structures on a paper substrate using inkjet-printing technology," *IEEE Transactions on Microwave Theory and Techniques*, vol. 55, pp. 2894 – 2901, 2007.

[10] J. A. Gordon, C. L. Holloway, J. Booth, S. Kim, Y. Wang, J. Baker-Jarvis, and D. R. Novotny, "Fluid interactions with metafilms/metasurfaces for tuning, sensing, and microwave-assisted chemical processes," *Physical Review B*, vol. 83, no. 20, p. 205130, 2011.

[11] A. Tidar, S. Shafiyoddin, S. Kamble, G. M. Dharne, S. S. Patil, P. W. Khirade, and S. Mehrotra, "Microwave dielectric relaxation study of 1-hexanol with 1-propenol mixture by using time domain reflectometry at 300k," in *Applied Electromagnetics Conference (AEMC), 2009*, Dec 2009, pp. 1–4.

[12] R. Nigmatullin, M. A.-G. Jafar, N. Shinyashiki, S. Sudo, and S. Yagihara, "Recognition of a new permittivity function for glycerol by the use of the eigen-coordinates method," *Journal of Non-Crystalline Solids*, vol. 305, pp. 96 – 111, 2002. [Online]. Available: http://www.sciencedirect.com/science/article/pii/S0022309302011250

[13] K. Shibata, "Measurement of complex permittivity for liquid materials using the open-ended cut-off waveguide reflection method," in *Microwave Conference Proceedings (CJMW), 2011 China-Japan Joint*, April 2011, pp. 1–4.

[14] T. Chretiennot, D. Dubuc, and K. Grenier, "A microwave and microfluidic planar resonator for efficient and accurate complex permittivity characterization of aqueous solutions," *Microwave Theory and Techniques, IEEE Transactions on*, vol. 61, no. 2, pp. 972–978, 2013.

[15] A. Catenaccio, Y. Daruich, and C. Magallanes, "Temperature dependence of the permittivity of water," *Chemical physics letters*, vol. 367, no. 5, pp. 669–671, 2003.